ATLAS PUB Note

ATL-PHYS-PUB-2019-011

29th March 2019
Minor revision: 3rd June 2019

Performance of tracking and vertexing techniques for a disappearing track plus soft track signature with the ATLAS detector

The ATLAS Collaboration

Several theories beyond the Standard Model predict the existence of massive long-lived charged particles with an extremely compressed mass spectra. This note presents improved tracking techniques for searches of long-lived charged particles decaying to a low momentum charged particle and a massive weakly interacting particle within the tracking volume of the ATLAS inner detector. This signature is characterized by a disappearing high momentum track with as few as three hits in the innermost layers of the ATLAS pixel detector, a low momentum charged track reconstructed in the outer layers of the ATLAS micro-strip tracker, and a displaced secondary vertex formed by the combination of these two tracks. Dedicated tracking and vertexing algorithms are developed to target this challenging signature, and the performance of these algorithms are characterized using a supersymmetric higgsino model, where the lightest chargino ($\tilde{\chi}_1^{\pm}$) is nearly degenerate with the lightest neutralino ($\tilde{\chi}_1^0$), and decays primarily $\tilde{\chi}_1^{\pm} \rightarrow \pi^{\pm}\, \tilde{\chi}_1^0$.

Revised based on the version released on 29th March 2019: reference [1] added.

1 Introduction

Several theories Beyond the Standard Model (BSM) predict the existence of massive long-lived charged particles with extremely compressed mass spectra [1, 2]. When the lifetime of such particles is of $O(0.01)$ ns to $O(10)$ ns, the charged state can decay to a low momentum charged particle and a neutral weakly interacting particle within the ATLAS inner detector (ID), leading to a "disappearing track signature". Searches for such particles have been performed by the ATLAS Collaboration in the past [3, 4] by reconstructing the short track using at least four hits in the innermost layers of the ATLAS pixel detector, and enforcing missing hits along the tracks trajectory in the outermost detector layers. Such tracks are referred to as disappearing *pixel tracklets*.

The specific BSM model studied in this note originates from a supersymmetric scenario where the lightest electroweak superpartner states are assumed to be "pure higgsino". In this scenario, the higgsino mass scale $|\mu|$ is very light with respect to other electroweak gaugino mass scales: $M_1, M_2 : |\mu| \ll M_1, M_2$. In this decoupled limit, the mixing of the higgsino eigenstates and other electroweak gaugino eigenstates is minimal, and four of higgsino states masses, $\tilde{\chi}_1^0$, $\tilde{\chi}_1^\pm$, $\tilde{\chi}_2^0$, are all degenerate at leading order. The mass splitting between $\tilde{\chi}_1^\pm$ and $\tilde{\chi}_1^0$ is produced dynamically through Standard Model loop corrections and is on the order of a few hundred MeV. The two lightest neutralino states are assumed to be mass degenerate. The primary decay mode of the long-lived chargino is $\tilde{\chi}_1^\pm \rightarrow \pi^\pm \tilde{\chi}_1^0$, where the charged pion has momentum on the order of the mass splitting between the chargino and neutralino states. Contributions to the decay width from electron and muons is less than 5% and depends on the mass splitting between the chargino and neutralino states. The lifetime of a $\tilde{\chi}_1^\pm$ decaying to $\tilde{\chi}_1^0$ and an associated charged particle is given by:

$$c\tau[\text{mm}] \sim 7 \times \left[\left(\frac{\Delta m\left(\tilde{\chi}_1^\pm, \tilde{\chi}_{1,2}^0\right)}{340\ \text{MeV}}\right)^3 \sqrt{1 - \frac{m_{\pi^\pm}^2}{\Delta m\left(\tilde{\chi}_1^\pm, \tilde{\chi}_{1,2}^0\right)^2}}\right]^{-1} \tag{1}$$

where $\Delta m\left(\tilde{\chi}_1^\pm, \tilde{\chi}_{1,2}^0\right)$ is the mass splitting between the chargino and neutralino states and $m_{\pi^\pm}$ is the mass of the charged pion. For chargino masses ranging from 150 GeV to 1000 GeV, the mass splitting ranges from approximately 280 MeV to 350 MeV leading to charginos with $c\tau \sim 14$ mm to 7 mm. At collider based experiments such as the Large Hadron Collider (LHC), the charginos can be pair produced or produced in association with the lightest two neutralino states as shown in Figure 1, and often are produced with significant momentum leading to a considerably longer apparent length of the chargino track making it possible to detect such scenarios.

Previous searches for long-lived supersymmetric charged particles searched for events with a disappearing pixel tracklet with at least four pixel hits, a high momentum jet, and large missing transverse momentum generated by the weakly interacting stable $\tilde{\chi}_1^0$ particles. These searches primarily focused scenarios where the favored lifetimes of the chargino is approximately a factor of four or more than the pure higgsino states. The results were interpreted in a pure higgsino scenario, but given the smaller higgsino production rates and relatively long length of track used in previous searches, sensitivity only extended up to 152 GeV [4] for the pure higgsino case. In order to improve on these results, significant developments are needed to improve the tracking techniques needed for shorter lifetime scenarios.

The tracking methods discussed in this note serve to improve upon the previously established techniques by extending their use to shorter tracks with fewer hits in the innermost pixel detector. These techniques are

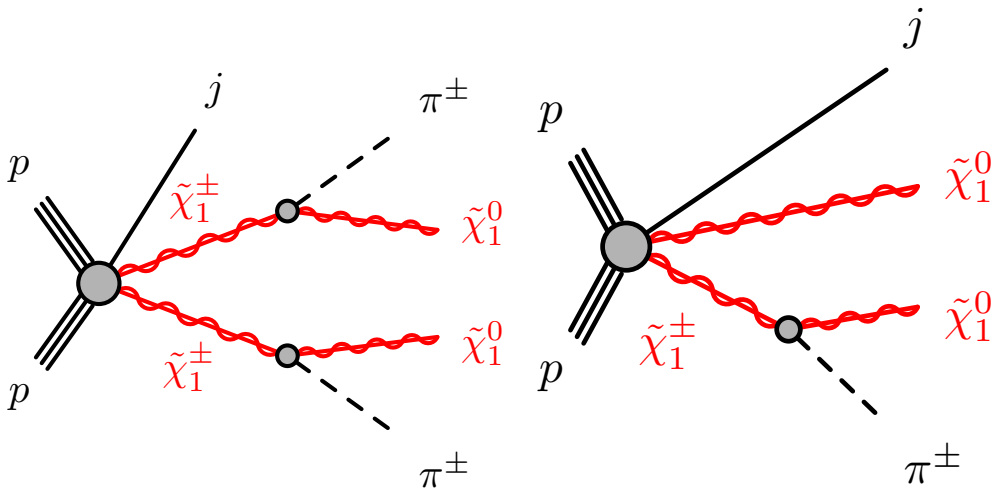

(a) (b)

Figure 1: Diagrams of the two production modes in a higgsino supersymmetric model used to characterize the tracking and vertexing techniques discussed in this note.

described in Section 5. As a consequence of having fewer hits along the tracklets trajectory, backgrounds arising from random combination of pixel hits increase significantly. To reduce these backgrounds, the low momentum charged particle emitted during the chargino decay is reconstructed, and a secondary vertex is formed between the chargino pixel tracklet and the soft-track to estimate the decay position of the chargino. The soft-tracking techniques are described in Section 6 and the secondary vertexing techniques are discussed in Section 7. This final state serves as a unique signature to search for pure higgsino states, and could be used to search for any signature with a charged particle decaying to one or more charged tracks within the tracking detector.

2 ATLAS detector

The ATLAS detector [5] is a multipurpose particle detector with a forward-backward symmetric cylindrical geometry and nearly 4π coverage in solid angle[1]. The inner tracking detector (ID) consists of silicon pixel and micro-strip detectors covering the pseudorapidity region $|\eta| < 2.5$, surrounded by a transition radiation tracker with coverage up to $|\eta| < 2.0$. A 2 T magnetic field oriented parallel to the beam axis causes charged particles to bend in the transverse plane (r–ϕ), and allows a measurement of the particles momentum. The magnetic field is generated by a solenoid magnet and surrounds the entire ID.

The pixel detector has four barrel layers extending up to a radius of 122.5 mm and three end-cap disks covering up to $z = \pm 650$ mm. The innermost pixel layer is called the insertable b-layer (IBL) [6, 7], and

[1] ATLAS uses a right-handed coordinate system with its origin at the nominal interaction point in the center of the detector. The positive x-axis is defined by the direction from the interaction point to the center of the LHC ring, with the positive y-axis pointing upwards, while the beam direction defines the z-axis. Cylindrical coordinates (r, ϕ) are used in the transverse plane with ϕ being the azimuthal angle around the z-axis. The pseudorapidity η is defined in terms of the polar angle θ by $\eta = -\ln\tan(\theta/2)$.

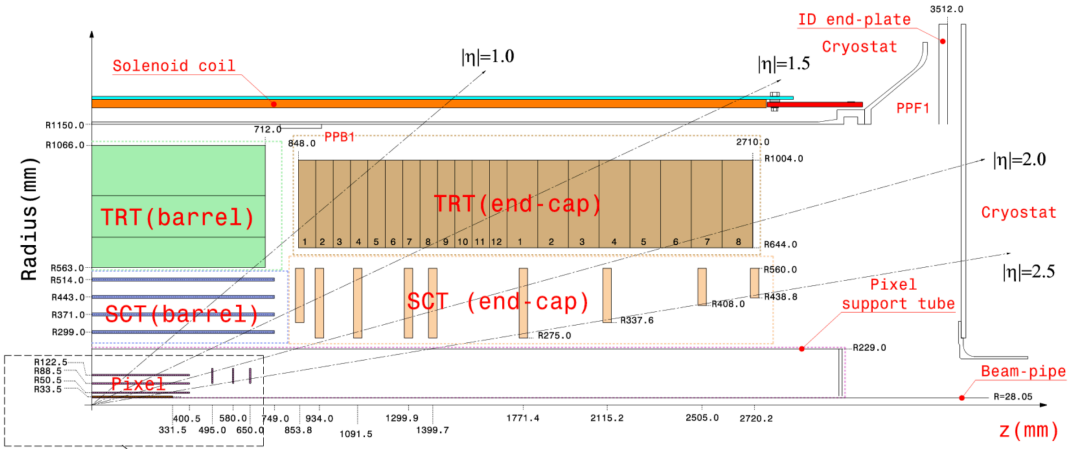

Figure 2: Schematic view of inner detector layout.

was added to the ATLAS detector in 2014 prior to Run 2 at a radius of 33.5 mm. The IBL has a reduced pixel size of 50 $\times$ 250 μm^2 compared to the outer pixel layers which have pixel sizes of 50 $\times$ 400 μm^2. The length of the pixel is oriented along the z-axis to allow precision measurements in the bending plane. The semiconductor tracker (SCT) encloses the pixel detector with four barrel layers of silicon microstrip detectors extending in radius from 299 mm to 514 mm, and nine end-cap disks with coverage up to $z = \pm 2720$ mm. The sensors have a length of 12 cm and a pitch of 80 μm, with their length oriented along the z-axis in the barrel and extend radially in the end-cap to allow precision measurements in the bending plane of charged particles. Each SCT detector layer is double sided with one side rotated along its geometric center by 40 mrad to allow for three dimensional position measurements. The side aligned parallel to the z-axis is referred to the axial sensor, and the rotated side as the stereo sensor. A detailed schematic of the ATLAS ID and the position of all the silicon detector layers is shown in Figure 2.

3 Simulated event samples

The studies presented in this note are based on simulated Monte Carlo samples. Pure-higgsino signal samples are generated with the MG5_aMC@NLO 2.3.3 event generator [8] at leading order (LO), considering $\tilde{\chi}_1^\pm \tilde{\chi}_1^0$, $\tilde{\chi}_1^\pm \tilde{\chi}_2^0$, and $\tilde{\chi}_1^\pm \tilde{\chi}_1^\mp$ production modes, and including up to two extra partons in the matrix element. Events are passed to Pythia 8.212 [9] for parton showering and hadronization. The CKKW-L merging scheme [10] was applied to combine tree-level matrix elements with parton showers. The scale parameter for merging was set to a quarter of the mass of the lightest neutralino state. The Pythia A14 [11] set of tuned parameters with simultaneously optimized multi-parton interaction and parton shower parameters was used together with the NNPDF2.3LO [12] parton distribution function (PDF) set. Two benchmark points are chosen with chargino mass $m(\tilde{\chi}_1^\pm) = 95$ GeV and 200 GeV and mass splittings of $\Delta m\left(\tilde{\chi}_1^\pm, \tilde{\chi}_{1,2}^0\right) = 254$ MeV and 296 MeV, respectively.

Simulated samples were overlaid with simulated minimum-bias events to model pile-up. The average number of pp interactions was chosen to match the data taking conditions in 2015 and 2016 and ranged between 10 and 40. The response of the detector to particles was modeled with the full ATLAS detector simulation [13] which is based on Geant4 [14].

4 Standard track reconstruction

Track reconstruction in the inner detector can be divided into four main stages: track seeding, track finding, ambiguity solving, and the TRT extension. Only a brief description of the relevant reconstruction algorithms is described below. A more detailed description of the track finding procedure can be found in Ref. [15], and a detailed description of the ambiguity solving algorithms can be found in Refs. [15, 16].

In the track seeding stage, combinations of three space-points[2] from the SCT detector or pixel detector are used to seed the trajectory of the track. Approximate track parameters are computed for each track seed and used to select seeds consistent with originating from the primary pp collision region. Track seeds are required to pass transverse (d_0) and longitudinal (z_0) impact parameter requirements with respect to the average position of the pp interactions (beam spot) [17], as well as minimum transverse momentum p_{T} requirements on the track seed. The standard track reconstruction algorithms require the impact parameter to be $|d_0| < 10$ mm and $|z_0| < 250$ mm, and the transverse momentum $p_{\mathrm{T}} > 500$ MeV.

The track seeds are then used as input for the track finding stage, where the track seed is used to initiate a search for additional hits along its trajectory in order to find complete tracks. A Kalman filter is used to follow the trajectory of the track candidate and include successive hits that satisfy χ^2 requirements between the hit and predicted trajectory position. The track parameters are progressively updated when propagating to the next detector element. In cases where the search fails to find any hit satisfying the χ^2 requirements on the next detector element, a hole is assigned to the trajectory. A maximum of two holes are allowed along the trajectory. Once no additional hits are found the track extension is terminated, and the final track is required to have a minimum of seven silicon hits to be accepted as a track candidate.

The track finding generates a large number of track candidates whose hits are often shared among different tracks. In order to resolve the ambiguity of which hits belong to which tracks, tracks are scored based upon their momentum, detailed hit information, number of shared hits, and length of their trajectory, and those tracks accepted by the ambiguity solving algorithm are then fit in a global chi-squared fit. Finally, tracks are extrapolated into the TRT detector and any hits compatible with the tracks trajectory are assigned to the final track candidate.

5 Pixel tracklet reconstruction

The majority of charginos will decay before passing through enough detector layers to satisfy the requirement of at least seven silicon hits in the standard track reconstruction described in Section 4. In the pure higgsino scenario the chargino's decay length ranges from 7 mm $\lesssim c\tau \lesssim$ 14 mm, which requires a relatively large Lorentz boost factor to leave a sufficient number of hits in the pixel detector to reconstruct the tracklet. In order to reconstruct as many charginos as possible across a wide range of lifetimes, the shortest possible track is desired. Since a helical trajectory in 3-dimensions needs at least three measurements to seed its trajectory, the minimum track length that's possible extends out to the third pixel layer (88.5 mm). This section describes the dedicated tracking configuration implemented to reconstruct tracklets with as few as three pixel hits. An efficient track extension is developed for this configuration to allow the reconstruction of longer tracks with additional pixel or SCT hits.

[2] A space-point is defined as a measurement in the pixel detector or the combination of axial and stereo layers in the SCT detectors. Hits are defined as measurements in the pixel, SCT or TRT detector. A hole is defined as a missing hit on an active module from the particles trajectory.

The reconstruction of pixel tracklets is performed as a "second-pass tracking" after the standard tracking is executed. In the second pass tracking, hits that have been used in tracks during the standard track reconstruction are masked and unavailable during the track seeding and track finding stages of the pixel tracklet reconstruction. The inefficiency of masking these already used hits was studied and found to result in less than 5% of inefficiency for chargino decays before the SCT layers. Decays within the SCT detector typically contain enough hits to be reconstructed by the standard track reconstruction algorithms with high efficiency after the second layer of the SCT detector, and therefore such tracks are unaffected by the second pass tracking.

The tracklets trajectory is seeded using three space-points formed in the pixel detector only. The SCT detector is not used to generate seeds for tracklets since short tracklets originating from the primary pp interaction are targeted. Chargino tracks with enough hits to be seeded using SCT space-points will be already efficiently reconstructed in the standard track reconstruction stage. All layers of the pixel barrel and end-cap detectors are available for the tracklet seeding. Once a track seed is formed, it's required to pass the same impact parameter requirements applied during the standard track reconstruction. Track seeds are required to have a minimum transverse momentum of $p_{\mathrm{T}} > 5$ GeV and $|\eta| < 2.2$. The tracklet seeding parameters are summarized in Table 1.

Table 1: Requirements on tracklet seeds. All impact parameters are measured relative to the beam spot.

Seed property	Requirement
Number of space-points	= 3
Transverse impact parameter	$\lvert d_0 \rvert < 10$ mm
Longitudinal impact parameter	$\lvert z_0 \rvert < 250$ mm
Minimum transverse momentum	$p_{\mathrm{T}} > 5$ GeV
Maximum pseudorapidity	$\lvert \eta \rvert < 2.2$

The pixel tracklet seeds are extended into track candidates by performing a search for additional pixel or SCT hits along its trajectory. As done for the standard track reconstruction, a road of detector elements is formed and the track parameters of the seed are propagated to the next detector element and compared with hits found on that element. The χ^2 between the hits and expected track position is required to be less than 15. In cases of multiple hits satisfying this criteria, the one with the smallest χ^2 is chosen. No holes along the trajectory are allowed. Once no additional hits are found, the outward track propagation is terminated. Tracks are accepted by the ambiguity solving algorithm using the same classification as the standard track reconstruction, except the minimum number of hits is relaxed to three, and none of the hits are allowed to be shared with any other track.

In the presence of multiple pp interactions in a given bunch crossing, a large number of hits will be produced in the detector that will not be assigned to a reconstructed track and will remain available to all second pass tracking algorithms. Since these hits generally have a poor compatibility with a full length track, they are rejected with high efficiency in the standard track reconstruction but remain available to all second pass tracking algorithms. In cases where the chargino decays before the SCT detector volume, it was found that the fraction of surviving tracklets that had at least one fake hit[3] was approximately 20% as shown in Figure 3. This background rate is dominated by single SCT hits (e.g. only a hit on its axial layer)

[3] A fake hit is defined to be any hit that does not originate from the chargino.

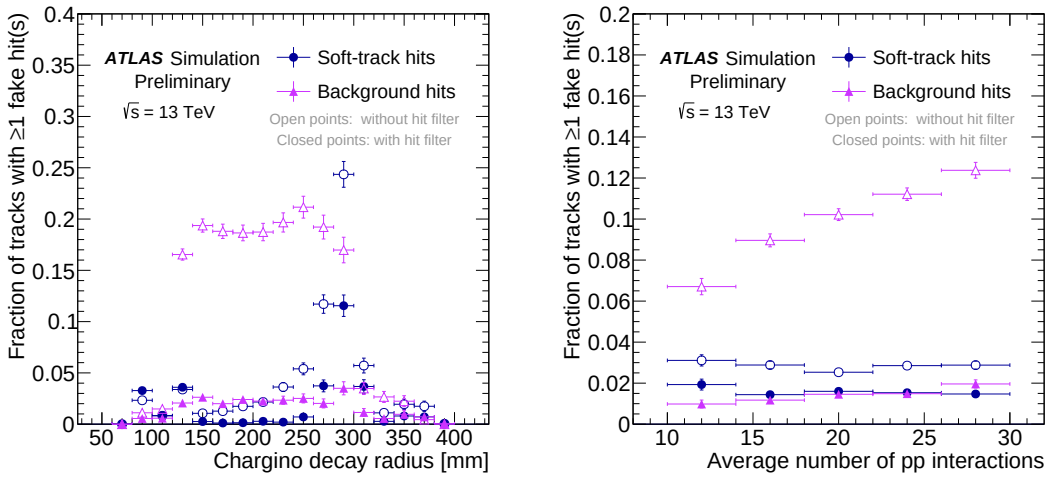

(a) (b)

Figure 3: The fraction of tracks with at least one fake hit from backgrounds or the soft-track as a function of the chargino decay radius (a) and the average number of *pp* interactions (b). Backgrounds include pile-up, fake hits, and secondary particles from material interactions. The rates are shown separately with and without the SCT hit filter.

and steeply rises with the number of *pp* interactions. A smaller but non-negligible contribution of hits originating from the charged decay product of the chargino is observed when the decay is close to an SCT layer. Although these tracks survive all the reconstruction stages, they would be vetoed during analysis since the disappearing track condition is formed by a veto on any SCT hits, leading to significantly inefficiency for physics analyses. In addition to this veto inefficiency, these spurious hits caused an additional 25% of inefficiency during the track finding stage, since the track candidate was often rejected due to the poor compatibility of its other measurements with these fake hits.

In order to recover this inefficiency, a SCT hit filter was introduced to remove these spurious hits. The filter was applied during the outward track extension stage and requires:

- Remove single SCT hits when the second-to-last measurement was on a pixel layer. This helps to reduce the effect of attaching single fake SCT hits when propagating from the last pixel layer into the SCT detector.
- When the last two hits are on SCT elements, require that they are on the same layer and are composed of stereo and axial measurements. Since no holes are allowed along the tracklet's trajectory, this helps to reduce cases where a single hit on a layer is attached to a trajectory with existing SCT hits.

The filter significantly improves the reconstruction efficiency and acceptance of tracks that satisfy the disappearing track condition by over 40%. In addition, it was confirmed to not affect the tracking efficiency by more than 5% when the chargino decay is truly within the SCT detector volume. The rate of fake SCT hits associated when this filter is applied was reduced to approximately the 2% level as shown in Figure 3, and is stable as a function of the number of *pp* interactions up to the level of 1%.

5.1 Chargino reconstruction efficiency

The efficiency to reconstruct a chargino was assessed using the benchmark signal samples discussed in Section 3. No significant differences in the reconstruction efficiency is observed between the two benchmark signal samples, and therefore the $m(\tilde{\chi}_1^{\pm}) = 95$ GeV point is chosen to evaluate the pixel tracklet performance for all studies in this section.

The reconstruction efficiency is defined as the number of tracks matched to a generated chargino over the total number of generated chargino particles:

$$\epsilon_{\text{reco}}(\tilde{\chi}_1^{\pm}) = \frac{\text{number of charginos matched to a reconstructed track}}{\text{number of generated chargino particles}}. \tag{2}$$

A hit-based truth matching scheme is performed to match reconstructed particles to generator level particles. A weighted truth matching score[4] is calculated for each reconstructed track, and the generator level particle with the highest weighted scored is considered matched to a reconstructed track if this weighted score is greater than 0.5. Although a relatively loose requirement is placed on this matching score, over 99% of pixel tracklets with only pixel hits have a matching score of 1 indicating a high purity of chargino hits contributing to the tracklets measurements.

The reconstruction efficiency is evaluated in the fiducial region of $|\eta| < 2.2$ to match the requirements applied during the tracklet seeding stage. A combination of the standard tracking and pixel tracklet reconstruction configurations are used to evaluate the efficiency, where the former has good efficiency for chargino decays beyond the second layer of the SCT detector when enough hits are left by the chargino, and the latter is designed to reconstruct much shorter tracks with high efficiency when the chargino decays before the SCT detector layers. The efficiency is studied both with an SCT hit veto and SCT hit requirement by cutting on the number of pixel and SCT hits, denoted n_{pix} and n_{SCT} respectively. The SCT veto efficiency requires $n_{\text{pix}} \geq 3$ and $n_{\text{SCT}} = 0$, and the SCT hit requirement requires $n_{\text{pix}} \geq 4$ and $n_{\text{SCT}} > 0$. The latter category can be used to search for longer lifetime charginos decaying within the SCT detector volume.

As shown in Figure 4, the average reconstruction efficiency across all decay positions is greater than 90%. Given the similar efficiency between the SCT veto and SCT hit requirement categories, no additional inefficiency is introduced with the SCT veto. This can be attributed to the SCT hit filter that was developed as part of this note, otherwise the SCT veto introduced up to 40% inefficiency for decays before the SCT detector volume. The efficiency is also shown as a function of the average number of pp interactions, where it can be seen that the efficiency is stable with only 5% of inefficiency between 10 and 40 pp interactions per bunch crossing. In this parameterization, the chargino decay radius is required to be 88.5 mm $< r <$ 300 mm and $r >$ 300 mm to select the fiducial detector volumes for the SCT veto and SCT hit requirement categories, respectively.

5.2 Impact parameter resolution

At the analysis level, pixel tracklets are selected with tight requirements on their impact parameters to help reduce contamination from tracklets formed from random hits in the pixel detector, collectively referred to as *fake tracklets*. Fake tracklets tend to have a uniform distribution of their impact parameters measured relative to the beam spot, while tracklets originating from the targeted SUSY process originate from the

[4] Pixel hits are assigned a weight of 10, SCT hits a weight of 5, and TRT hits a weight of 1. The score is normalized to unity.

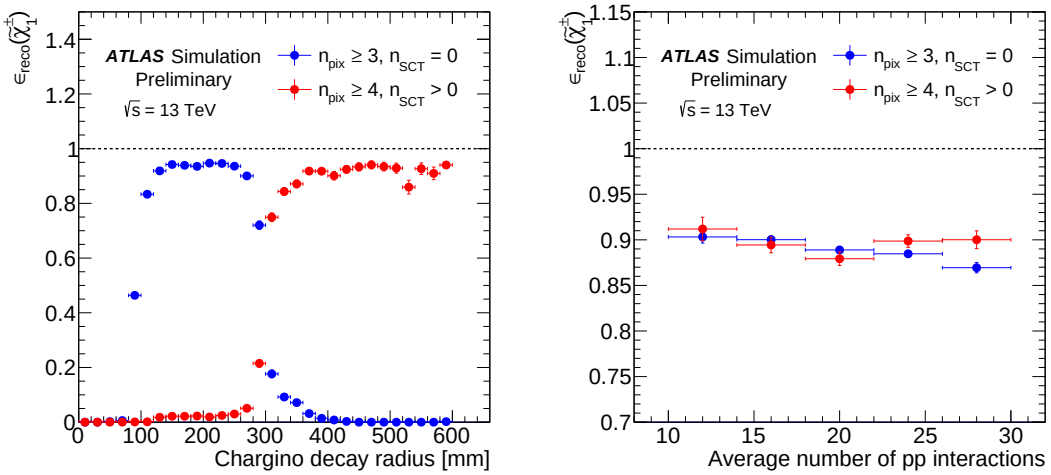

(a) (b)

Figure 4: The reconstruction efficiency for charginos as a function of the its decay position (a) and the average number of pp interactions (b). Figure 4(b) has fiducial volume requirements of 88.5 mm $< r <$ 300 mm and $r >$ 300 mm applied for the SCT veto and SCT hit requirement categories, respectively.

primary pp interaction. Due to the small number of measurements along the tracklet's trajectory, the impact parameter resolution can be significantly worse than standard tracks, especially for the transverse impact parameters which depends on the tracklet's curvature. The impact parameter resolution of the tracklets was quantified by studying the differences between the reconstructed and the generator level values at the perigee[5]. The true values of the impact parameters are extracted by propagating the generator level particle quantities at its production vertex to the beam spot. The resolution is then extracted by calculating the standard deviation of the distribution of the difference between the reconstructed and generator level impact parameters. The calculations are performed in bins of p_{T} and η, and the resolution is extracted and displayed as a function of these variables.

The impact parameter resolution is studied for different requirements on the number of pixel and SCT hits. Tracklets with $n_{\mathrm{SCT}} = 0$ are studied with $n_{\mathrm{pix}} = 3$ or $n_{\mathrm{pix}} \geq 4$, and are referred to as three and four hit tracklets respectively. Tracklets with $n_{\mathrm{pix}} \geq 4$ and $n_{\mathrm{SCT}} > 0$ hits are included for comparison and referred to as long tracklets.

The transverse and longitudinal impact parameter resolution as a function of the chargino's generator level p_{T} and η is shown in Figure 5. The transverse impact parameter resolution depends strongly on the measurement of the tracklets curvature (q/p_{T}), which generally scales as $\Delta p_{\mathrm{T}}/p_{\mathrm{T}} \propto 1/L_{\mathrm{T}}^2$, where p_{T} is the particles transverse momentum and L_{T} is the projected length of the track in the transverse plane. Due to the small number of measurements, the resolution for the three hit tracklets is expected to be significantly worse than the long tracks. The three layer transverse impact parameter resolution is found to be approximately a factor of two worse than the long tracklets.

The longitudinal impact parameter resolution shows a strong dependency on the η of the track due to

[5] The perigee is defined to be the point of closest approach to the beam spot.

the incident angle of the track relative to the detector surface. On average central tracks have pixel measurements from a single pixel, while the more forward tracks have multiple pixels contributing to their hit measurements due to the high incident angle of the track [18, 19]. The longitudinal hit size in the innermost pixel layer ranged from an average of one pixel at $\eta \sim 0$ and up to three pixels at $\eta \sim 2.2$. The effect of ganging together multiple pixels improves the single hit resolution along z and therefore leads to an improved longitudinal impact parameter resolution. The difference between the different hit categories is small except for the central most tracks, since the z pointing resolution is mainly driven by the presence of pixel layer measurements.

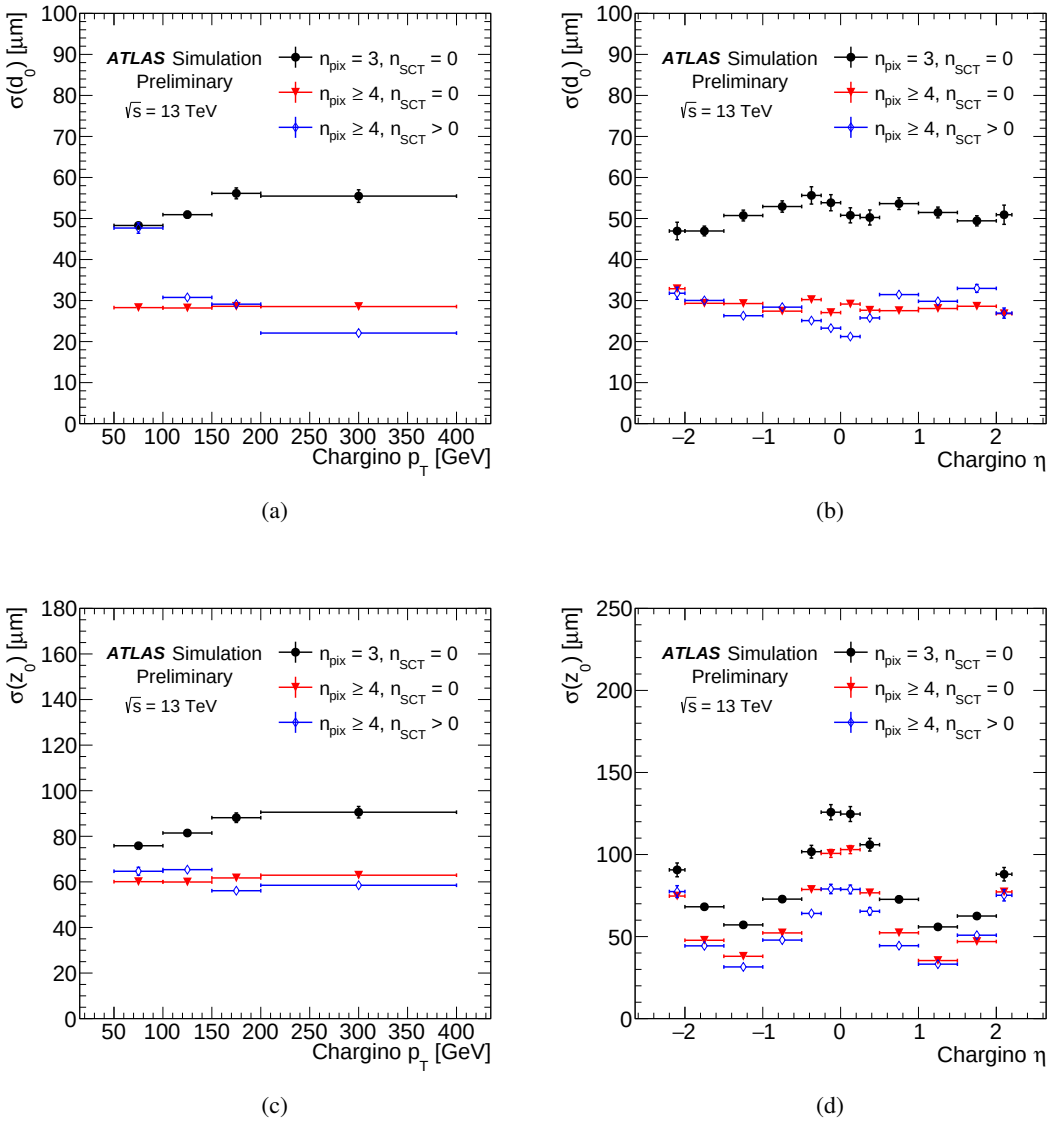

(a) (b)

(c) (d)

Figure 5: The transverse d_0 (a-b) and longitudinal z_0 (c-d) impact parameter resolution as a function of the generator level chargino p_{T} and η for different hit requirements on the tracks. n_{pix} and n_{SCT} are the number of pixel and SCT hits, respectively.

6 Soft-track reconstruction

The rate of fake tracklets tends to increase as the number of measurements along the tracklets trajectory decreases and therefore can be a significant background when reconstructing tracklets with only pixel hits. In order to reduce this background for pixel tracklets, the charged particle from decay of the chargino is targeted. Due to the small mass splitting between the chargino and neutralino states, this charged particle has extremely low momentum, ranging from approximately 250 MeV to 350 MeV for chargino masses between 95 GeV to 1000 GeV, and typically has large impact parameters measured relative to the beam spot. Clearly the minimum $p_{\mathrm{T}} > 500$ MeV and tight impact parameter requirements applied during the standard track reconstruction would reject the bulk of these particles, and therefore a dedicated configuration is required to reconstruct these charged particles.

6.1 Region of interest track seeding

A dedicated technique is developed for the seeding stage of the soft-track reconstruction to control the execution times, which would otherwise exceed the standard tracking execution time by over an order of magnitude. The soft-track reconstruction is run as a second pass tracking similar to the pixel tracklet reconstruction described in the previous section, and therefore only unused hits are available to the soft-track seeding algorithm. The seeding technique takes as input the pixel tracklets discussed in Section 5. The tracklets are required to have transverse momentum $p_{\mathrm{T}} > 20$ GeV, at least three pixel hits, no SCT hits, and are required to be isolated from other tracks in the event. The isolation is applied by summing the transverse momentum of all tracks with $p_{\mathrm{T}} > 500$ MeV around the tracklet candidate with $\Delta R < 0.4$, where $\Delta R \equiv \sqrt{\Delta\phi^2 + \Delta\theta^2}$, and requiring that this sum normalized by the tracklet p_{T} is less than 10%. The isolation requirement significantly reduces the executing time by ignoring soft-radiation produced during the hadronization of jets that would otherwise be ignored by the standard tracking algorithms due to the relatively high minimum p_{T} requirement. Finally the tracklets are ordered according to their d_0 to give priority to space-points matched to prompt tracklets.

Once the tracklets have been pre-selected, a region of interest (RoI) is created by selecting the outermost hit along the pixel tracklet. Using the beam spot as the origin, a pointing direction is defined. Space-points from the SCT detector are collected within a cone of $\Delta R < 0.8$ between the pointing direction of the tracklet and a given space-point in the SCT tracker. The $\Delta\phi$ and $\Delta\theta$ between all soft-track space-points and the last measurement along the tracklet is shown in Figure 6, showing that the majority of space-points down to a transverse momentum of 200 MeV are contained within an angular cone of $\Delta R < 0.8$. Combinations of three SCT space-points are required to have a minimum transverse momentum $p_{\mathrm{T}} > 200$ MeV. Instead of measuring the impact parameters from the beam spot, the origin is set dynamically to the last measurement along the tracklet, and the impact parameters are measured relative to this position. Since the last measurement is not necessarily the decay vertex of the chargino, somewhat loose requirements (but much tighter than using the beam spot as the origin) are applied to the seed candidate. The transverse impact parameter is required to be $|d_0^{\mathrm{pix}}|<150$ mm and $|z_0^{\mathrm{pix}}|<1000$ mm, where d_0^{pix} and z_0^{pix} are the transverse and longitudinal impact parameters measured relative to the last pixel measurement.

Track seeds are extended into full length tracks by performing a search for additional SCT hits along its trajectory. A minimum of six hits are required for the track to be accepted, and at least four of the hits along the extended track must not be shared with any other tracks. The total number of shared hits with any other tracks cannot exceed two hits, and along its trajectory a maximum of two SCT holes are allowed.

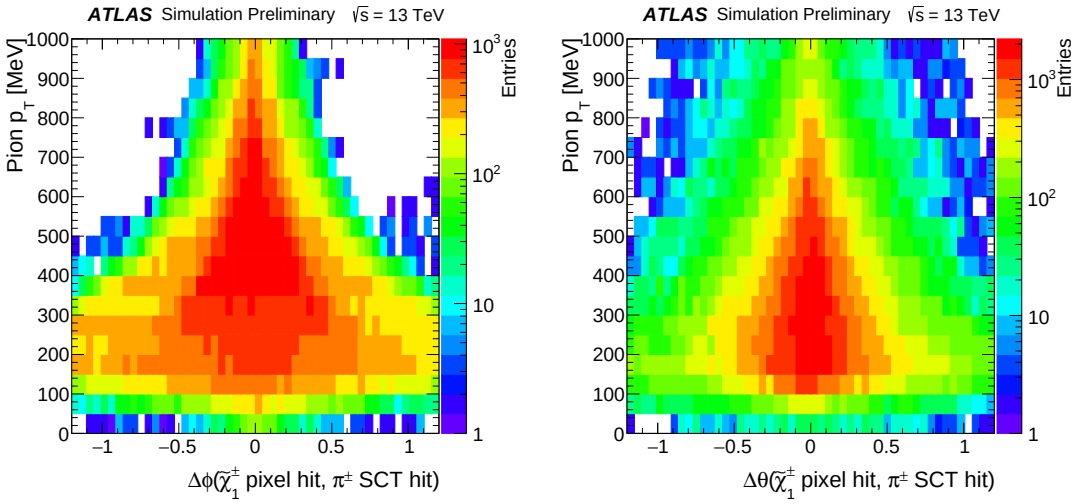

(a) (b)

Figure 6: The generator level soft-pion transverse momentum vs the $\Delta\phi$ (a) and $\Delta\theta$ (b) between the last pixel hit along the tracklets trajectory and all the SCT hits from the soft-pion originating from the chargino decay.

6.2 Soft-track reconstruction efficiency

The reconstruction efficiency was studied using both of the benchmark signal samples in Section 3. The definition of the reconstruction efficiency is the same as Eq. 2, but is evaluated after a tracklet was successfully reconstructed with the same requirements applied at the soft-track seeding level described in the previous section. Furthermore, the efficiency is evaluated for all soft-tracks[6] with a generator level $p_{\mathrm{T}} > 200$ MeV to match the requirements applied during the reconstruction.

The reconstruction efficiency as a function of the generator level p_{T}, transverse impact parameter d_0, its production radius, and the average number of pp interactions is shown in Figure 7. The efficiency as a function of the transverse momentum rises steeply and reaches $\epsilon_{\mathrm{reco}}^{\text{soft-track}} \gtrsim 50$–$60\%$ for tracks with $p_{\mathrm{T}} > 300$ MeV. The relaxed impact parameter requirements for the soft-track reconstruction extend the tracking efficiency out to $|d_0|$ of 150 mm with reasonably high efficiency, but tends to suffer from inefficiencies for the largest $|d_0|$ values due to the smaller number of hits expected when the decays are nearly parallel to the detector layers. The efficiency as a function of the production radius is approximately 60%, except for cases where the chargino decays beyond the first layer of the SCT detector ($r > 299$ mm) resulting in fewer SCT hits for the soft-track reconstruction, and when the chargino decays between the last two pixel layers (88.5 mm $< r <$ 122.5 mm). In the latter case, a 10% inefficiency arises when tracks are reconstructed by the standard tracking algorithms and penalized during the track scoring stage for missing hits on the innermost pixel layers. Finally, the efficiency is found to be reasonably robust against pile-up with only 10–20% inefficiency between the lowest and highest number of pp interactions explored in this sample. Efficiency can be lost in high pile-up environments when the standard tracking wrongly assigns hits from the soft-track to fake tracks reconstructed in the first pass, causing them to be masked for this dedicated reconstruction algorithm.

[6] Soft-tracks refer to any charged track (pion,electron, or muon) from the decay of the chargino.

Differences in efficiency between the two signal points arise from the different mass splitting of the two samples and the average momentum of the parent chargino particle. In the case of $m(\tilde{\chi}_1^{\pm})$ = 200 GeV, the soft-tracks have a slightly harder momentum spectrum than $m(\tilde{\chi}_1^{\pm})$ = 95 GeV, but receive less of a momentum boost resulting in more tracks with larger $|d_0|$ values. The efficiency for the $m(\tilde{\chi}_1^{\pm})$ = 200 GeV point when parameterized as a function of p_{T} is more enriched in larger d_0 tracks than $m(\tilde{\chi}_1^{\pm})$ = 95 GeV at lower momentum values, and therefore results in apparent efficiency losses as a function of p_{T}.

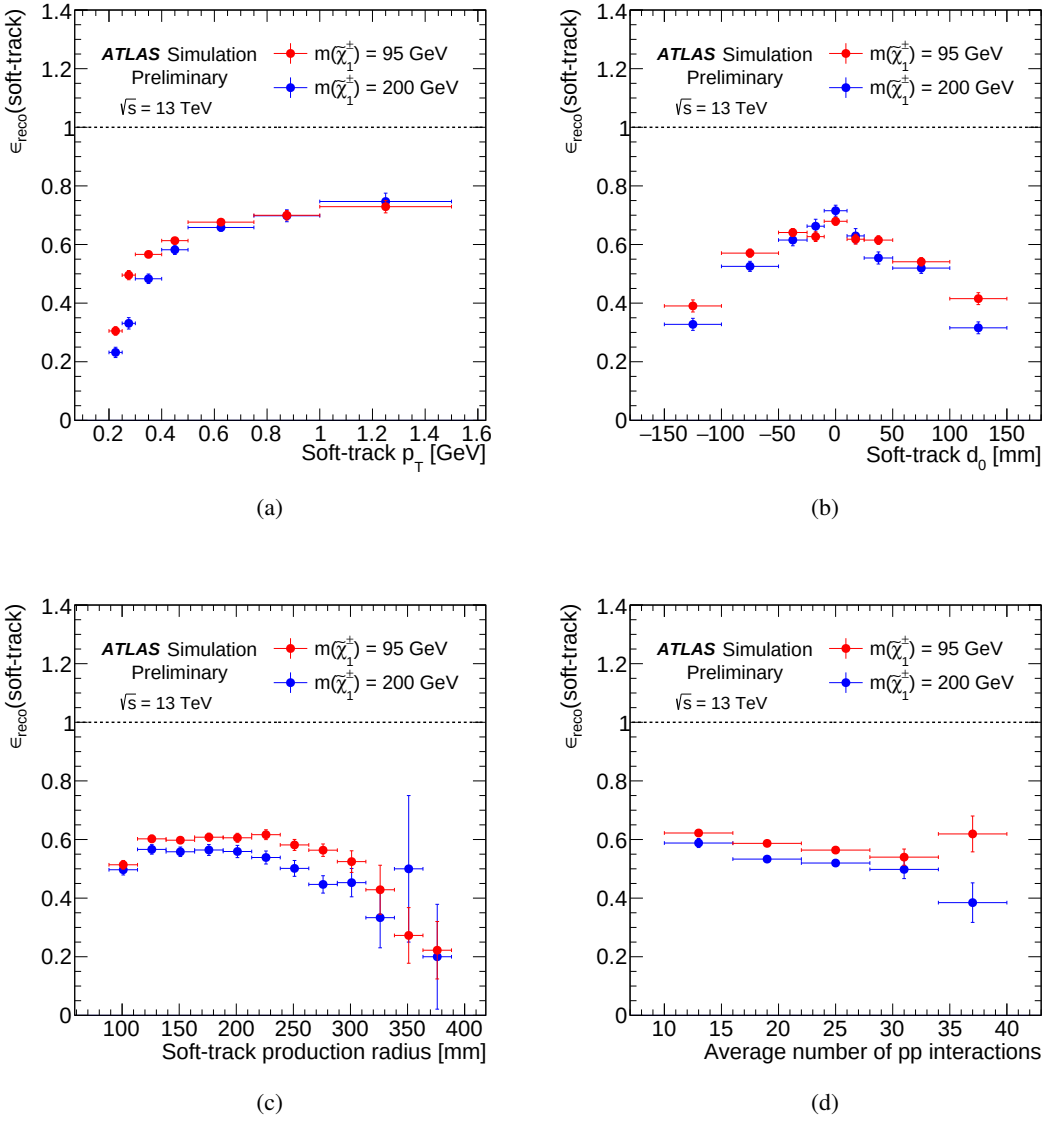

(a) (b)

(c) (d)

Figure 7: Soft-track reconstruction efficiency as a function of the generated soft-track p_{T} (a), transverse impact parameter (b), production radius, (c) and average number of pp interactions (d). All plots require the soft-track generator level p_{T}>200 MeV, soft-track production radius r > 88.5 mm, and the reconstruction of a chargino tracklet with the same requirements applied at the soft-track seeding level.

7 Vertex reconstruction

The tracklet and soft-track are combined in a two track vertex fit to estimate the decay position of the chargino. On an analysis level, the fitted vertex properties can be used to pair a pixel tracklet and soft-track by choosing the best-quality vertex fit, and can help to veto backgrounds originating from material interactions by vetoing vertex positions close to detector layers. This section describes the implementation of the vertex fit, its performance after track reconstruction, the position resolution of the reconstructed vertex, and the soft-track impact parameter resolution relative to the fitted vertex position.

Tracks are pre-selected before the vertexing is performed. Tracklets are required to have $p_{\mathrm{T}} > 20$ GeV and at least three pixel hits. An SCT hit veto is applied to the pixel tracklet to define the disappearing track condition and to allow the soft-tracks to utilize all layers of the SCT detector for their reconstruction. Due to the poor impact parameter resolution of the tracklets in the central regions, tracklets are required to have $|\eta| > 0.1$. The soft-track is required to have 200 MeV $< p_{\mathrm{T}} <$ 1500 MeV with at least six SCT hits and a maximum of one pixel hit, where a veto on the innermost two pixel layers is enforced.

A two track vertex fit is attempted for all combinations of pixel tracklets and soft-tracks whose angular distance is less than 1.5. The vertex fit follows closely the techniques described in Ref. [20], and is distinguished into a *fast* and *full* vertex fit. Both fits approximate the equations of motion of a charged particle in a magnetic field to first-order in a Tayler expansion in terms of (q/p), where $q = \pm 1$ is the charge of the particle, and p is its momentum. The fast vertex fit is used to estimate the initial position of the vertex. It drops any correlations of the vertex position with the track momenta. This initial position is used as a constraint in the full vertex fit.

Vertices fit with the full vertex information are required to have a $\chi^2 / n_{\mathrm{dof}} < 10$, where n_{dof} is the number of degrees of freedom in the fit. In addition, sanity requirements are placed on the vertex radius and it's required to be 85 mm $< r <$ 300 mm, corresponding to roughly the fiducial volume spanned between the third pixel barrel layer and first SCT barrel layer.

7.1 Vertex reconstruction efficiency

The vertex reconstruction efficiency is computed as the number of reconstructed chargino-decay vertices over all generated vertices, after requiring the successful reconstruction of both the chargino and soft-track, such that the tracking efficiency is factored out. A reconstructed vertex is defined as one where both reconstructed tracks are truth matched to the tracklet and soft-track:

$$\epsilon_{\mathrm{vtx}} = \frac{N_{\mathrm{truth}}(\text{vertex reconstructed} \mid \text{seed tracks reconstructed})}{N_{\mathrm{truth}}(\text{seed tracks reconstructed})} \tag{3}$$

where N_{truth} is the number of generated vertices under the conditions of having their decay products reconstructed as tracks. In order to enter the numerator, the generated vertex has to have a corresponding reconstructed vertex whose constitute tracks are truth matched to the chargino and soft-track.

The vertex reconstruction efficiency as a function of the chargino decay radius, the average number of pp interactions, the soft-track d_0, and the ΔR(chargino, soft-track) between the chargino and soft-track is shown in Figure 8. The efficiency is found to be robust against multiple pp interaction and shows a small dependency on the chargino's decay position. A small inefficiency is observed for small d_0 values,

corresponding to scenarios where the chargino and soft-track are collinear. In such situations, the vertexing becomes difficult since in the limit of exactly parallel tracks the intersection has no well defined solution. This effect can be seen clearly as a function of the ΔR(chargino, soft-track), where the efficiency is plotted as a function of the opening angle between the chargino and soft-track. At small opening angles, an inefficiency is observed.

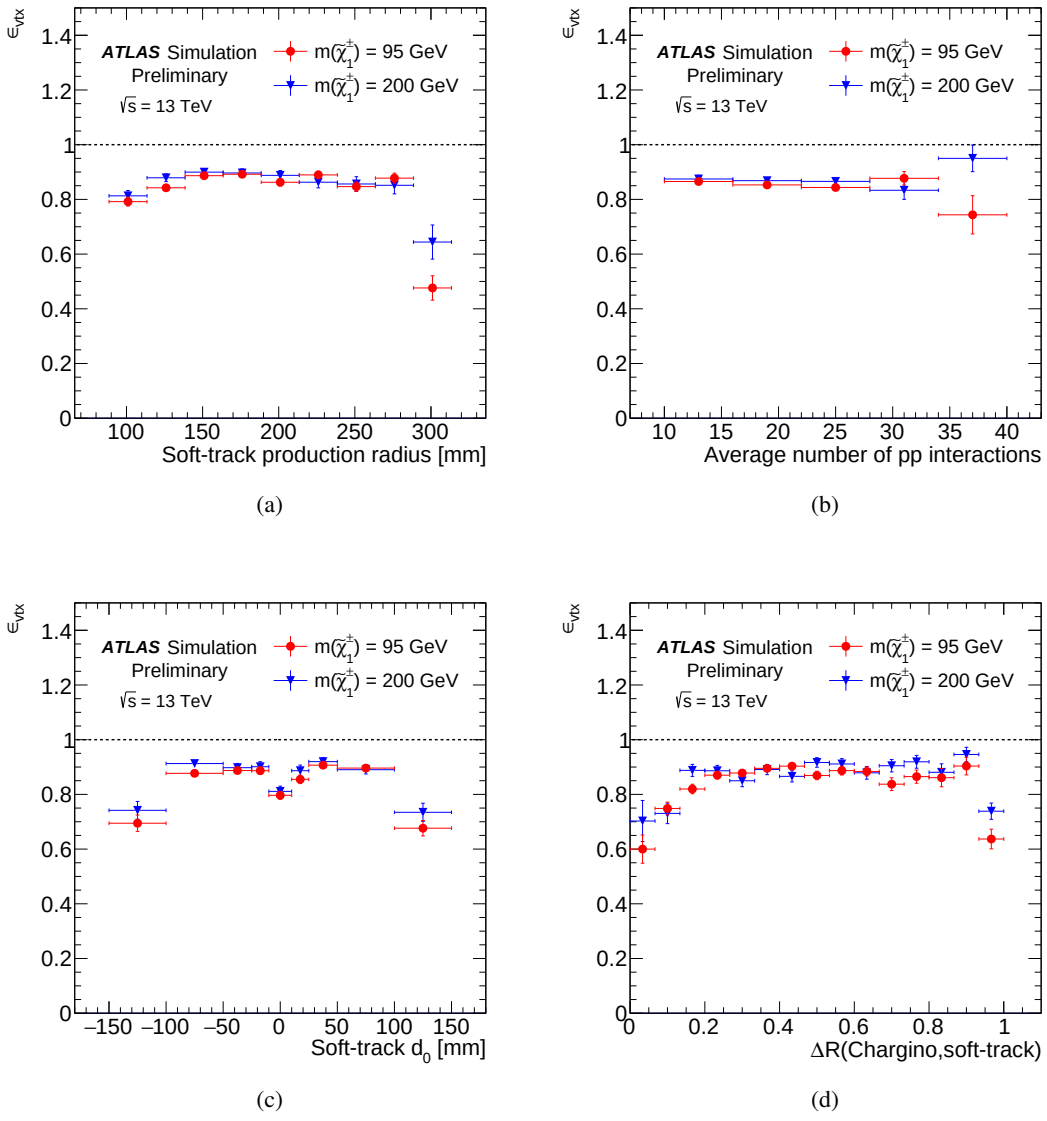

Figure 8: Vertex reconstruction efficiency as a function of the soft-track production vertex position (a), the average number of pp interactions (b), the soft-track d_0 (c) and the ΔR(chargino,soft-track) (d). The efficiency is calculated after the successful reconstruction of the chargino and soft-track.

7.2 Vertex position resolution

The vertex position resolution was studied as a function of the x,y and z position coordinates. It is evaluated for decay positions between 0 mm $< r <$ 150 mm and 150 mm $< r <$ 300 mm, correspondingly roughly to cases where the track parameters from the SCT only track are extrapolated to inside or outside the pixel volume, respectively. Since the majority of tracks originate from the dedicated soft-track reconstruction without any pixel measurements, it's expected that the position resolution will degrade the further the track parameters are extrapolated from the SCT detector.

The resolution is extracted by fitting a double Gaussian distribution to the difference between the generator level and reconstructed vertex position. The generated vertex position is taken as the decay position of the chargino. One Gaussian is used to model the core distribution and another for the long tails, where the latter is constrained to have a larger width than the core distribution, but both share a fully correlated mean value. The necessity of two models for the core and tail originates from the mixture of opening angles between the chargino and soft-track trajectories: when the two trajectories are nearly parallel, finding the intersection of their trajectories becomes a challenging problem compared to when there is a large opening angle between the two tracks. The latter situation has a much better position resolution than the former case.

An example of the fitted distributions are shown in Figure 9 for x and z coordinates in the fiducial region of $r <$ 150 mm and 150 mm$< r <$ 300 mm, respectively. The resolution along the x and y directions are comparable, since the pixels and SCT strips are oriented to have the best possible hit resolution in the x–y bending plane. Along the z coordinate the core resolution is approximately 650 μm, but has a large contribution in the tails where the resolution can be up to 5 times worse than the core resolution. Since the SCT strips are orientated along the z-axis, it's expected that the pointing resolution will be worse along z than the coordinates in the bending plane. The resolutions for each coordinate and two separate radial selections of the detector are summarized in Table 2.

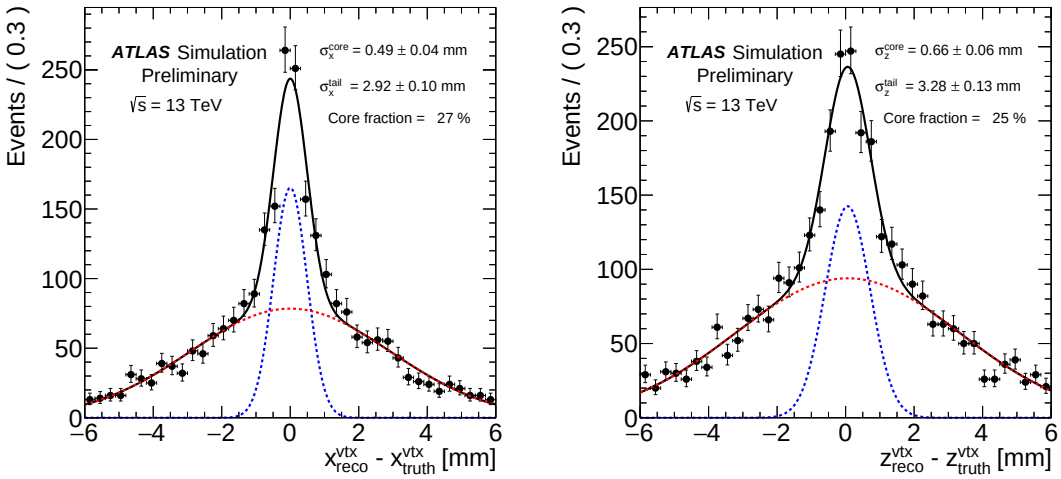

(a) $r <$ 150 mm (b) 150 mm$< r <$ 300 mm

Figure 9: Two example vertex position resolution fits for the x (a) and z (b) coordinates in two different radial regions of the detector. The resolution is extracted using two Gaussian distributions to model the core and tails of the resolutions.

Table 2: Vertex position resolution for the core and tails of the the vertex reconstruction. The resolutions are shown separately for x,y and z coordinates, and for two different radial (r) regions of the detector. The numbers in the parentheses show the fraction of events fitted in the core and tails of the distribution.

	$r < 150$ mm	150 mm $< r <$ 300 mm
σ_x^{core}	0.49 ± 0.04 mm (27%)	0.52 ± 0.03 mm (38%)
σ_x^{tail}	2.92 ± 0.10 mm (73%)	2.41 ± 0.06 mm (62%)
σ_y^{core}	0.49 ± 0.07 mm (22%)	0.52 ± 0.03 mm (33%)
σ_y^{tail}	2.86 ± 0.10 mm (78%)	2.36 ± 0.05 mm (67%)
σ_z^{core}	0.65 ± 0.08 mm (18%)	0.66 ± 0.06 mm (25%)
σ_z^{tail}	3.69± 0.20 mm (82%)	3.28 ± 0.13 mm (75%)

7.3 Secondary vertex impact parameters

The track parameters measured relative to the secondary vertex position can be a useful tool for physics analysis. For a genuine $\tilde{\chi}_1^{\pm} \rightarrow \pi^{\pm} \tilde{\chi}_1^0$ decay, tight requirements can be placed on the secondary vertex impact parameters to enforce compatibility of the tracks with originating from the secondary vertex, while rejecting a large amount of fake soft-tracks spuriously associated to a fake tracklet.

The track parameters were propagated to the position of the secondary vertex using both the generator level and reconstructed track parameters in order to study the secondary vertex impact parameter resolution of the soft-track. The resolution was extracted in bins of the reconstructed soft-track p_{T} and η, as well as the fitted vertex radius, using the same method described in Section 5.2.

The transverse and longitudinal impact parameter resolution as a function of the fitted vertex radius is shown in Figure 10. The resolution shows a strong dependence on the radius of the reconstructed vertex, since most tracks originate from the dedicated soft-track reconstruction configuration using only SCT detector elements and the pointing resolution degrades as the track parameters are extrapolated further from the hit measurements in the SCT.

The secondary vertex d_0 and z_0 impact parameter resolution for the soft-track were also studied as a function of the generator level soft-track p_{T} and η as shown in Figure 11. At such low momentum, the effects of multiple scattering become large and significantly degrade the resolution towards lower momentum. Since the majority of tracks use only hits in the SCT detector, the resolution degrades towards large η since the pointing direction of the SCT becomes worse into these forward regions due to the strip orientation.

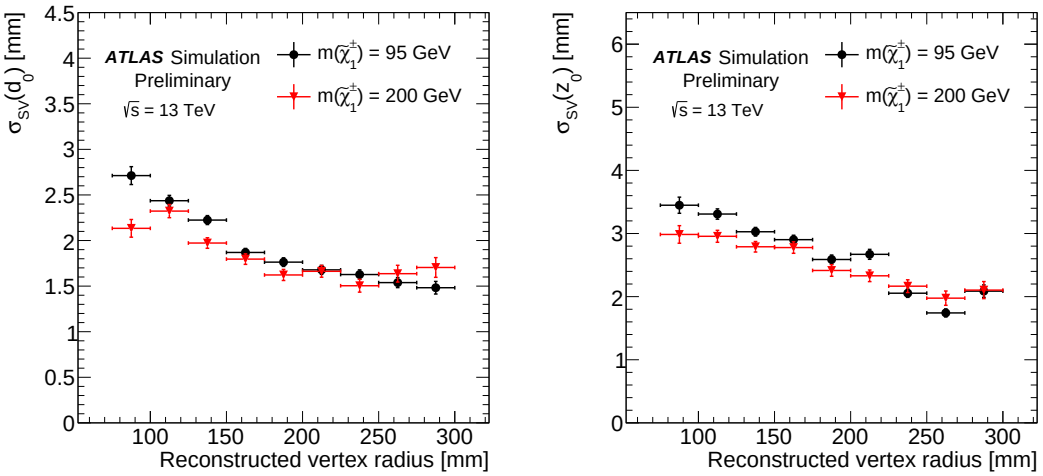

(a) (b)

Figure 10: Transverse (a) and longitudinal (b) impact parameter resolutions of the soft-tracks measured relative to the fitted secondary vertex position, as a function of the vertex radius.

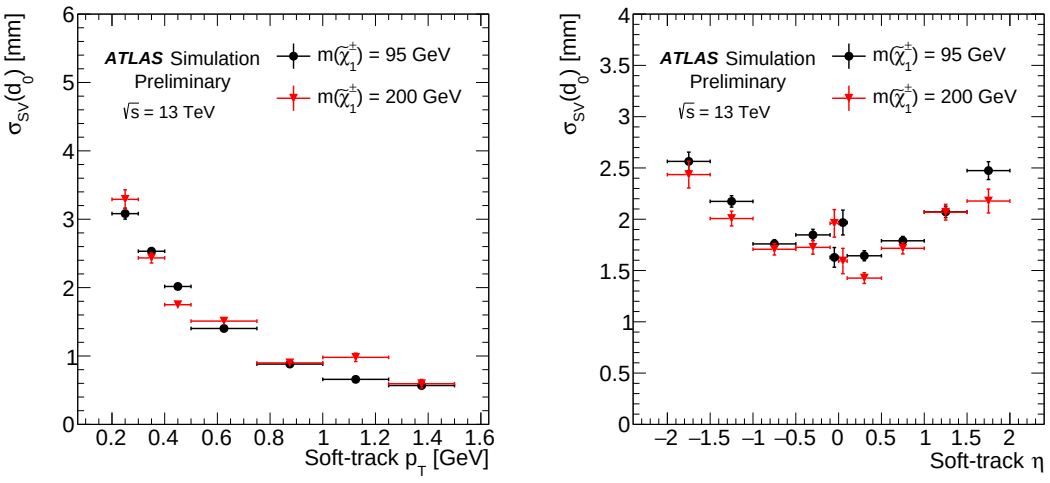

(a) (b)

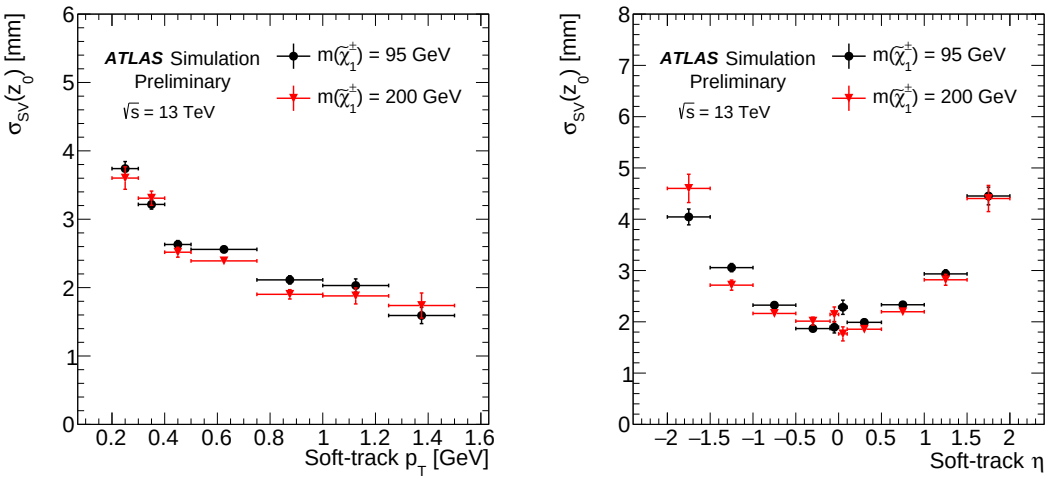

(c) (d)

Figure 11: Transverse (a, b) and longitudinal (c, d) impact parameter resolutions of the soft-track relative to the fitted secondary vertex position, as a function of the generator level soft-track p_T and η.

8 Conclusion

Techniques for reconstructing short *pixel tracklets* with as few as three pixel hits and an extremely low momentum charged track produced with significant displacement from the primary pp interaction was presented. The performance of these techniques were characterized using a pure supersymmetric higgsino model, where the next-to-lightest state is the chargino decaying to the lightest neutralino and a low momentum particle. These techniques are expected to serve as a unique signature and significantly improve sensitivity in searches for pure higgsinos using the ATLAS detector.

The efficiency to reconstruct tracklets was shown to be greater than 90% for decays beyond the third pixel layer, and was shown to be robust against multiple pp interactions due to the development of a dedicated SCT hit filter. The soft-track reconstruction was performed using a region of interest technique whereby the pixel tracklet is used to seed a search for SCT space-points around the last pixel measurement in the seed tracklets trajectory. These techniques reduced computation time by over an order of magnitude and achieve an efficiency of greater than 60% for soft-tracks with $p_{\mathrm{T}} > 300$ MeV. The two-track vertex efficiency for the combination of the pixel tracklet and soft-track was shown to be greater than 90% when both tracks are successfully reconstructed, except for cases where the soft-track is produced with very small or large impact parameters. The core vertex position resolution was evaluated by comparing the reconstructed vertex properties to the charginos decay position, and found to be approximately 500 μm and 650 μm in the transverse and longitudinal direction, respectively.

References

[1] R. Mahbubani, P. Schwaller and J. Zurita,
Closing the window for compressed Dark Sectors with disappearing charged tracks,
JHEP **06** (2017) 119, [Erratum: JHEP10,061(2017)], arXiv: 1703.05327 [hep-ph].

[2] H. Fukuda, N. Nagata, H. Otono and S. Shirai, *Higgsino Dark Matter or Not: Role of Disappearing Track Searches at the LHC and Future Colliders*, Phys. Lett. **B781** (2018) 306,
arXiv: 1703.09675 [hep-ph].

[3] ATLAS Collaboration, *Search for long-lived charginos based on a disappearing-track signature in pp collisions at* $\sqrt{s} = 13$ *TeV with the ATLAS detector*, JHEP **06** (2018) 022,
arXiv: 1712.02118 [hep-ex].

[4] ATLAS Collaboration,
Search for direct pair production of higgsinos by the reinterpretation of the disappearing track analysis with 36.1 fb^{-1} *of* $\sqrt{s} = 13$ *TeV data collected with the ATLAS experiment*, (2017),
URL: http://cds.cern.ch/record/2297480.

[5] ATLAS Collaboration, *The ATLAS Experiment at the CERN Large Hadron Collider*,
JINST **3** (2008) S08003.

[6] ATLAS Collaboration, *ATLAS Insertable B-Layer Technical Design Report*,
ATLAS-TDR-19 (2010), URL: https://cds.cern.ch/record/1291633;
ATLAS Insertable B-Layer Technical Design Report Addendum, ATLAS-TDR-19-ADD-1 (2012),
URL: https://cds.cern.ch/record/1451888.

[7] ATLAS IBL Collaboration, *Production and Integration of the ATLAS Insertable B-Layer*,
JINST **13** (2018) T05008, arXiv: 1803.00844 [physics.ins-det].

[8] J. Alwall et al., *The automated computation of tree-level and next-to-leading order differential cross sections, and their matching to parton shower simulations*, JHEP **07** (2014) 079, arXiv: 1405.0301 [hep-ph].

[9] T. Sjöstrand et al., *An Introduction to PYTHIA 8.2*, Comput. Phys. Commun. **191** (2015) 159, arXiv: 1410.3012 [hep-ph].

[10] L. Lonnblad and S. Prestel, *Matching Tree-Level Matrix Elements with Interleaved Showers*, JHEP **03** (2012) 019, arXiv: 1109.4829 [hep-ph].

[11] ATLAS Collaboration, *ATLAS Pythia 8 tunes to 7 TeV data*, (2014), URL: https://cds.cern.ch/record/1966419.

[12] NNPDF Collaboration, R. D. Ball et al, *Parton distributions for the LHC Run II*, JHEP **04** (2015) 040, arXiv: 1410.8849 [hep-ph].

[13] ATLAS Collaboration, *The ATLAS Simulation Infrastructure*, Eur. Phys. J. **C70** (2010) 823, arXiv: 1005.4568 [physics.ins-det].

[14] S. Agostinelli et al., *GEANT4: A simulation toolkit*, Nucl. Instrum. Meth. A **506** (2003) 250.

[15] ATLAS Collaboration, *Performance of the ATLAS Silicon Pattern Recognition Algorithm in Data and Simulation at $\sqrt{s}$ = 7 TeV*, (2010), URL: https://cds.cern.ch/record/1281363.

[16] ATLAS Collaboration, *The Optimization of ATLAS Track Reconstruction in Dense Environments*, (2015), URL: https://cds.cern.ch/record/2002609.

[17] ATLAS Collaboration, *Reconstruction of primary vertices at the ATLAS experiment in Run 1 proton–proton collisions at the LHC*, Eur. Phys. J. **C77** (2017) 332, arXiv: 1611.10235 [physics.ins-det].

[18] ATLAS Collaboration, *A neural network clustering algorithm for the ATLAS silicon pixel detector*, JINST **9** (2014) P09009, arXiv: 1406.7690 [hep-ex].

[19] ATLAS Collaboration, *Training and validation of the ATLAS pixel clustering neural networks*, (2018), URL: http://cds.cern.ch/record/2309474.

[20] P. Billoir and S. Qian, *Fast vertex fitting with a local parametrization of tracks*, Nucl. Instrum. Meth. A **311** (1992) 139.